Representing space in time during ocular drift

August 7, 2014

How is space represented in the visual system? In an immobile eye, a stationary stimulus is necessarily encoded by the pattern of active receptors in the retina. But, the eyes are always in motion, even during fixation, and eye movements make spatial information available in the temporal domain. Our recent work has provided strong evidence that the visual system also uses the temporal modulations resulting from fixational eye movements to encode fine spatial detail (Rucci et al., 2007; Kuang et al., 2012). Here we investigated the mechanisms of this encoding process. Subjects viewed a standard Vernier stimulus in complete darkness through a narrow vertical aperture, which allowed exposure of only one line at a time. They reported whether the top line was to the left/right of the bottom one. The aperture was stabilized on the retina, so that no spatial cues existed on the retina and the exposure of the two lines was solely determined by ocular drift (trials with saccades/microsaccades were discarded). To successfully perform this task, knowledge of eye movement was necessary, as the temporal pattern on the retina was, by itself, ambiguous. We conducted three separate experiments. In the first experiment, stimuli were presented on a fast CRT monitor. In the second experiment, to rule out possible contributions from the CRT phosphor persistence, stimuli were delivered by an array of ultra-fast LEDs. In the third experiment, we used a different technique for retinal stabilization in which stimuli were viewed through deflecting mirrors. Results were similar in all experiments: performance was significantly above chance with offsets of a few arcminutes. These results reveal that spatial information exclusively contained in the temporal structure of fixational modulations suffices to discriminate fine patterns, even in the absence of spatial displacements.

Introduction

How is space represented in the visual system? At first sight, the answer to this question may appear straightforward. Since the optics of the eye forms an image on the retina, space is naturally represented by the activity of cells with receptive fields at different locations within the visual field. However, an alternative possibility also exists. The eyes are always in motion during the periods in which visual information is acquired and processed, and this

motion transforms spatial information in the temporal domain. Thus, space can also be represented by temporal changes in the neural activity.

With externally-moving stimuli, it has long been known that temporal modulation can indeed be interpreted as spatial cues (Barlow, 1979; Burr, 1979; Burr and Ross, 1986; Morgan, 1979). A large body of evidence suggests that the perception of spatial detail originates from delays in neural responses with such stimuli (*e.g.*, Brenner and Smeets, 2000; Krekelberg and Lappe, 1999; Purushothaman et al., 1998; Schlag and Schlag-Rey, 2002; Whitney and Murakami, 1998).

But even stimuli stationary in space actually move on the retina because of fixational eye movements. Can temporal modulations caused by fixational eye movements contribute to spatial perception? In the present work, we investigated whether fine spatial detail can be represented in time by means of the modulations resulting from one component of fixational eye movements: the slow ocular drift that incessantly moves the eyes in the periods in between saccades. This hypothesis builds on a long history (Hering, 1899; Averill and Weymouth, 1925; Marshall and Talbot, 1942). Recent theoretical studies (Ahissar and Arieli, 2001, 2012) have reformulated old proposals within the context of current knowledge on the visual system and experimental studies have given support to the idea that fixational eye movements contribute to fine spatial vision (Rucci et al., 2007; Kuang et al., 2012).

More specifically, the experiments of the present study were designed to investigate whether the visual system has access to the extra-retinal knowledge of ocular drift and uses this information in the establishment of spatial representations. This proposal may appear to contradict multiple previous findings. For example, Poletti et al. (2010) recently subjects easily get confused in the establishment of spatial representations, something that should not happen with the contribution of an extra-retinal drift signal. In this experiment, observers were asked to report in a two forced-choice-task which one of two test dots briefly presented during ocular drift was at the same spatial location of a reference marker presented at the beginning of a trial. The presentations of the stimuli were separated by 500 ms intervals, and test markers were displayed at the same location of the reference either on the display or on the retina. Results showed that the larger the extent of ocular drift, the higher the probability of making a mistake, reporting the test marker displayed at the same retinal location of the reference as the one displayed at its same spatial location. Thus, these results suggests that in the absence of visual references the brain ignores changes in the eye position caused by ocular drift.

Studies aimed at investigating the limits of visual acuity (*e.g.*, Westheimer and Hauske, 1975) also suggest that possible extra-retinal signals related to eye drift are not used by the visual system. In many tasks, the ability of the visual system to discriminate fine patterns goes far beyond the limits imposed by the layout of retinal photoreceptors, a phenomenon known as hyperacuity. Westheimer and Hauske (1975) studied how acuity changed when the two elements of a Vernier pattern (a stimulus often used to study hyperacuity) were not displayed simultaneously. Matin et al. (1981) showed that when the two lines of a Vernier stimulus were flashed sequentially, sensitivity to the Vernier offset deteriorated with the duration of the interstimulus interval. The results suggest that the deterioration displacements caused by involuntary eye movements during the interstimulus blank interval are not compensated by the visual system.

Although the results of the studies described above show that the visual system does not integrate the extra-retinal information into the percept, this information may be still available in the visual system and used under different circumstances. Arathorn et al. (2013) recently examined perceptual compensation of ocular drift. They asked observers to report the perceived motion of stimuli under different retinal motion conditions using a matching task. The results showed that the perceived stability of images moving in a direction consistent with motion held for a range of amplitude motions. However, objects moving with different gains were perceived stable with respect to each other. They argued that the visual system compensate for the retinal slip induced by eye motion.

Here, we investigated whether human observers are capable of discriminating fine spatial patterns that purely exist in the temporal domain because of ocular drift. In a two forced-choice task, observers were asked to report whether the top line of a Vernier stimulus was on the left or on the right of the bottom line. The two lines were never visible simultaneously and their relative position depended on the observer's eye movements –specifically the way in which the eye drifted. Retinal stabilization allowed us to eliminate the retinal offset between the two lines, so that no spatial cue was available to the visual system to perform the task.

Results of the present study strongly suggest that in the absence of explicit spatial information, cues encoded in the temporal domain seem to be sufficient for establishing spatial representations. These results indicate that the visual system has knowledge of the direction of ocular drift and uses this knowledge to establish coherent spatial representation.

Materials and methods

Subjects

A total of 6 observers with normal, non-corrected vision participated in the study. All observers, with the exception of one of the authors, were naïve about the purposes of the experiment.

Stimuli and Procedure

Data were collected in separate experimental sessions, each of approximately one hour duration. Every session started with preliminary setup operations that lasted a few minutes and allowed the subject to adapt to the low level of light in the room. Preliminary operations included: (1) positioning the subject optimally and comfortably in the apparatus; (2) tuning the eye tracker; and (3) performing a calibration procedure to convert the voltages given by the eye tracker into degrees of visual angle. These operations were also repeated before each block of trial. A dental imprint bite line and a head rest prevented movements of the head.

The movements of the right eye were measured by means of a Generation 6 Dual Purkinje Image (DPI) eye tracker (Fourward Technologies). The internal noise of this system is about 20" (Crane and Steele, 1985), enabling a spatial resolution of eye movement of approximately 1' (Stevenson and Roorda, 2005). Vertical and horizontal eye positions were sampled at 1 KHz and recorded for subsequent analysis. Stimuli were observed monocularly, with the left eye patched.

In all three experiments, observers faced the same task. They were asked to report whether the top line of a Vernier stimulus was to the right or to the left of the bottom line. The stimuli was viewed though a narrow aperture that was stabilized with the eye of the observer, allowing the exposure of only on line at a time (Fig. 5a).

Experiment 1

A total of 6 observers participated in Experiment 1. Figure 6a summarizes the experimental procedure of this experiment. Stimuli were displayed on a fast phosphor monitor (Iyamaya HM204DT) at a resolution of 1024×768 pixels and vertical refresh rate of 200 Hz.

The lines forming the Vernier stimulus were 1.35' wide and 28.35' long and the vertical gap between them was

8' (Fig. 5). Both lines were displayed on the retina at the same position on the horizontal axis (the Preferred Retinal Locus of Fixation, PRLF). The duration of the exposure of the each line varied according to the eye movements of the observers: the line remained visible until the line of sight moved away from it. Then, after 100 ms, the second line of the Vernier stimulus was shown at the same horizontal retinal position of the first line and it remained visible as long as the line of sight was at that particular location. The order of presentation of the two lines was random. At the end of each trial, a bright random noise mask was presented for 1333 ms to signal to the observer the conclusion of the trial and avoid dark adaptation.

To ensure accurate localization of the line of sight, at the beginning of each block of trials, observers were asked to perform a calibration procedure. This procedure consisted of two phases. In the first phase (automatic calibration), subjects sequentially fixated on each of the 9 points of a 3×3 grid, as is standard in oculomotor experiments. In the second phase (manual calibration), subjects confirmed or refined the voltage-to-pixel mapping given by the automatic calibration. In this phase, they fixated again on each of the points of the grid, while the location of the line of sight estimated on the basis of the automatic calibration was displayed in real time on the screen. Subjects used a joypad to correct its position, if necessary. These corrections were then incorporated into the voltage-to-pixel transformation. This procedure was repeated every 5 experimental trials for the central marker only, to compensate for possible drifts in the eye tracker and ensure precise positioning of the stimuli on the retina throughout the course of the experimental session.

Experiment 2

Although Experiment 1 was designed to avoid explicit spatial cues, two cues may have occurred: (1) motion on the stimulus on the retina because of the finite steps of retinal stabilization and (2) the persistence of the phosphors on the CRT. These cues may leave an undesired spatial trace of the configuration of the Vernier stimulus. To circumvent this problem, we designed a second experiment (Experiment 2) in which stimuli were displayed for much shorter intervals on a custom-made discrete LED display specifically designed to minimize phosphor persistence. Figure 13 summarizes the experimental procedure of this experiment, in which 3 observers participated. The display consisted of 880 LEDs, each of the dimension of 0.2×0.5 mm, organized in two main rows, each containing columns of 110 LEDs. A line was created by turning on 4 LEDs in a column. At the distance

of the display from the observer, each line was 1.75' wide and 17.5' long and the vertical gap between lines was 4.38' (Fig. 5a).

In a trial, each line was displayed on the retina, aligned vertically with the PRLF, for 20 ms only. Then, after 100 ms, the second line of the Vernier stimulus was shown at the same horizontal retinal position of the first line and it remained visible again for 20 ms. The order of presentation of the two lines was random.

Like in Experiment 1, at the beginning of each block of trial, observers performed a two-phases calibration procedure, which enabled precise localization of the line of sight. In the first phase, subjects sequentially fixated on each of 9 small LEDs arranged in a 3×3 grid, an approach similar to that of Experiment 1. In the second phase, observers confirmed or refined the voltage-to-pixel mapping given by the first phase of calibration by adjusting the horizontal position of a line displayed on the top row of the LED monitor, while fixating on a line displayed at the center of the bottom row of the LED monitor. The top line was stabilized on the retinal and observers used a joypad to adjust its position. Like in Experiment 1, this refinement was repeated every 5 experimental trials.

Experiment 3

The experimental procedure of Experiment 3 is the same as Experiment 2, but here stimuli were displayed for shorter intervals (5 ms). The blank interval duration tested in Experiment 3 could be either 100 or 500 ms. This two conditions were run in different sessions.

Experiment 4

To ensure that imperfections in retinal stabilization did not give explicit spatial information, we also designed a third experiment, which used a different technique for retinal stabilization. In this experiment (Experiment 4), we used a stimulus deflector (see Crane and Clark, 1978) to stabilize the stimulus on the retina. Stimuli were displayed on a fast CRT monitor as in Experiment 1 (Iyamaya HM204DT). A total of 2 observers participated in this experiment.

Figure 19 summarizes the experimental procedure used in Experiment 4. In this experiment, each line was displayed in a position vertically aligned with the preferred retinal locus of fixation, for 20 ms. The interstimulus time interval was either 100 or 500 ms. The order of presentation of the two lines (bottom or top) was random.

Because of the different apparatus, the calibration procedure of Experiment 4 differed from those of the pre-

vious two experiment. Since the stimulus deflector stabilizes the entire visual field, it does not allow an approach similar to the one in Experiment 1. For this reason, before positioning the stimulus deflector, we first estimated the position of the line of sight by presenting a stabilized cue at the center of the CRT display, and a grid of 9 unstabilized crosses. These 9 markers were physically positioned before the first mirror of the stimulus deflector to remain at a fixed (unstabilized) spatial location. Observers first aligned the stabilized cue with the central marker of the unstabilized grid while fixating on this marker. To achieve this alignment, the observer used two knobs that controlled the horizontal and vertical offset of the stabilized cue. These controls rotated the horizontal and vertical mirrors of the stimulus deflector. Once the offset was eliminated, the gain of the deflector was adjusted by making saccades towards the unstabilized markers. If the unstabilized marker did not overlap with the unstabilized one, the observer changed the gain of the stimulus deflector and repeated the procedure.

We then used an after-image to further refine the calibration. We presented to the observer a stabilized high contrast line (10×50 pixels) at the center of gaze during sustained fixation. After 10 s, a time sufficient to develop an after-image, the observer made saccades toward the peripheral unstabilized marker. If, after the saccade, the observer perceived a negative after-image — a black line— the gain of the stimulus deflector was changed. This operation was repeated until the bright, stabilized line overlapped with the dark, after-image one. The observer was instructed to adjust the gain of the stimulus deflector until the dark line remained “hidden behind” the bright one as he/she moved his/her eyes back and forth. The observer moved the line of sight at the central unstabilized marker and repeated the procedure while making saccades toward at different peripheral unstabilized markers. The 9 crosses grid was removed at the end of the calibration procedure.

The calibration procedure was very time consuming. This, together with the need for high cooperation from the observer, limited the window of time available for data acquisition and only allowed collection of data from 2 experienced observers in this experiment.

Figure 5b compares the presentations of the stimuli on the display and on the retina in the three experiments. To clarify the differences, two examples of eye movements are shown. Both move the eye towards the right, but EM_1 has a downward drift whereas EM_2 has an upward drift. As clarified by the figure, no spatial cue was present in any of the experiments. In Experiment 2, although the stabilized lines were vertically aligned with the PRLF, the gaze contingent display did not allowed stabilization on the vertical axis. In the two scenarios presented in

Figure 5b, eye movements changed the displacement between the two lines: in the case of EM_2 the two lines fully overlapped on the retina, stimulating the same receptors but at different times. On the display, a horizontal offset between lines was present in Experiment 1 and 2 but not in Experiment 4. In Experiment 4 no spatial offset was ever present either on the display or on the retina no matter the eye movement performed by the observer. This was an advantage of Experiment 4: it allowed exposure to high contrast stimuli stabilized on both the horizontal and vertical axes while excluding possible spatial cues resulting from phosphor persistence.

Data analysis

Recorded eye movements traces were segmented into separate periods of drift and saccades. Classification of eye movements was performed automatically and then validated by human experts. Periods of blinks were automatically detected by the DPI eye-tracker and removed from data analysis. Only trials with optimal, uninterrupted tracking, in which the fourth Purkinje image was never eclipsed by the pupil margin, were selected for data analysis.

Eye movements with minimal amplitude of 3' and peak velocity higher than 3^o/s were selected as possible saccades. Consecutive events closer than 15 ms were merged together into a single saccade, a method that automatically excluded the post-saccadic overshoots that may result from the movement of the lens and, possibly, the dampening of the eye-tracker (Deubel and Bridgeman, 1995; Stevenson and Roorda, 2005). Saccade amplitude was defined as the modulus of the vector connecting the two locations at which eye speed became greater (saccade onset) and lower (saccade offset) than 2^o/s. Saccadic rates were calculated over the entire duration of each trial. In this study, we do not distinguish between saccades and microsaccades; all saccadic movements are analyzed together independent of their magnitudes.

Periods, which were not classified as saccades or blinks, were automatically labeled as drifts. The data presented in this study consist of the trials in which no saccades occurred (the drift-only trials). Trials in which the observer was able to discriminate the relative position of the two lines were classified as correct.

Results

Experiment 1

To determine whether the visual system is capable of establishing spatial representations from delays in neuronal responses, we designed an experiment in which observers were asked to report the configuration of a standard Vernier viewed through a narrow aperture (Fig.5a). The two lines forming the Vernier were never visible at the same time, and their offset was exclusively determined by eye movements. This was achieved showing the two bars so that on the retina were vertically aligned with the Preferred Retinal Locus of Fixation (PRLF). The intervals in which the two bars were exposed were separated by a period of 100 ms. Since the eye drifted in this interval, the two lines were actually presented at different locations on the monitor (but at the same horizontal position on the retina). In this way the input to the retina did not contain any explicit spatial cue signaling the offset between the two lines (Fig. 6a).

Figures 6b shows an example of eye movement recorded in a trial. In this particular trial, the center of gaze moved leftward and the two bars were displayed in the intervals marked by the shaded regions. Figure 6c shows a 2D reconstruction of the trial as it appeared on the monitor. Subjects were asked to report the spatial configuration of the Vernier stimulus, that is whether the top bar was located to the left or to the right of the bottom one. If the visual system is not capable of reconstructing space from the temporal modulation resulting from ocular drift, subjects should not be able to perform this task, and discrimination performance are expected to be at chance levels.

The gap size between the two lines depended on the movement of the eye during the 100 ms blank interval. Figure 7 shows the 2D probability distribution of the gaze position during ocular drift periods in the 100 ms blank interval. The horizontal component of this motion determined the relative position of the two bars and represents the information that the visual system needs to encode in order to perform this task.

Figure 8 shows the instantaneous velocity and speed of ocular drift. In agreement with previous reports (Cherici et al., 2012), the instantaneous drift velocity showed varied across observers in an idiosyncratic manner. On average, the 2D speed of drift, was 53 ± 7 arcmin/s, a value within the range of ocular drift speed previously observed in experiment in which observers maintained sustained fixation on a small marker (Cherici et al., 2012).

The results of Experiment 1 for each observer are summarized Table I. Percentage of correct response, number of trial and correct trials, and confidence interval (CI) for a binomial distribution are reported in the table. Correct trials are the ones in which observers detected accurately the polarity (left/right) of the displacement between the two lines. Those are the trials in which the visual system correctly integrated a possible motion signal associated with ocular drift. The data show that already at gap size of 1.35', a microscopic displacement, the proportion of correct response was significantly higher than chance level in all observers ($p < 0.05$, CI for binomial distribution). Performance was also significantly higher than chance at gap size 2.7' ($p < 0.05$, for binomial distribution) and ranged from 77% to 87%. In 3 subjects the performance at gap size 2.7' was significantly higher than at gap size 1.35' ($p < 0.05$, paired t-test). The data of Table I are plotted graphically in Figure 9, which shows the proportion of correct response as a function of the gap size (*i. e.*, the displacement of the eye during the blank interval) for each observer. As previously noted, performance was higher than chance level at both 1.35' and 2.7' gap size for all observers.

Average data across observers are shown in Figure 10a. The average percentage of correct report across observers was 69% with a standard deviation of 6 at gap size 1.35'. Performance increased significantly to $84\% \pm 4$ when the displacement between the two lines also increased to 2.7' ($p = 0.0028$, paired t-test). Figure 10a also shows the average sensitivity index *d'* as a function of gap size. On average across observers, the *d'* was 0.99 at gap size 1.35' and it increased to 2.02 at gap size 2.7' reflecting the facility with which observers discriminated the stimuli.

Collapsing the data across observers revealed similar results. The performance, when there was no offset between the two lines, was 46% (CI: [0.36 0.55]), whereas at gap size 1.35' it increased significantly above chance level to 70% (CI: [0.67 0.74]). Increasing the gap size, the performance for the collapsed data also increased to 85% (CI: [0.82 0.88]). Finally, with gap size larger than 2.7', the performance was 79% (CI: [0.73 0.87]).

Even if the order of the presentation top/bottom line was randomized, the configuration of the two stimuli was dictated by the direction of ocular drift on the horizontal axis. It is therefore possible that the results were consequences of a combination of a general bias in the direction of ocular drift and a bias in the subject response: for example, the observer may not have access to an extra-retinal drift signal but have a general knowledge that his eye tends on average to drift in a given direction. For this reason, we analyzed performance as a function

of the direction of ocular drift. As shown in Figure 10b, the average performance across observers was similar for both direction of motion. This result demonstrate that our findings were not a consequence of biases toward a particular direction of ocular drift or in the response of observers. These results suggest that a Vernier offset can be detected accurately thanks to the information in the temporal domain even when spatial information is not available, and they support the hypothesis that the visual system has access to motor/proprioceptive information of the direction of motion of the eye during ocular drift periods.

We also examined whether the performance of the observers was affected by the speed of ocular drift or the duration of exposures. The average speed of ocular drift during the 100 ms blank interval was not significantly different between correct and wrong trials ($p = 0.2999$, paired t-test). Figure 11 shows that on average the duration of the exposure of the lines was significantly shorter in wrong trials ($p = 0.0108$, paired t-test). However, no significant differences were found between the exposure of the two lines within correct or wrong trials (correct trials: $p = 0.8538$, paired t-test; wrong trials: $p = 0.3330$, paired t-test).

One possible explanation of our findings is that stabilization errors contributed as spatial cues. Because of the way the stabilization was performed, the position of the eye, in arcmin, was converted in real time, during the experimental sessions, into pixels. This method only allows to stabilize stimuli with the granularity of the pixels of the monitor. That is, if the line of sight moved within a pixel size (1.35'), no change in the stabilized stimuli was implemented. In order to exclude this possibility, performance was studied as a function of stabilization errors, defined as the difference in the average residuals between the line of sight and the position of the stimuli. Figures 12 a and b show the proportion of response to the right as a function of the retinal error for each observers and the resulting average across observers. If the stabilization error affected the performance of the observer, the proportion of right response would be small for errors with negative values and high for positive errors. As shown in Figure 12b none of the observers showed such pattern, suggesting that the possible retinal caused by imperfections in the retinal stabilization did not affect performance. This results is also reflected in the average across observers as shown in Figure 12a.

A possible problem in this experiment is the decay time of CRT phosphors. After tuning a phosphor off, its brightness decays quickly to low levels but it does not achieve zero immediately. This decay property has been previously found to affect the performance in experiment ran to explore integration information across saccades

leading to false conclusions (Jonides et al., 1982; Irwin et al., 1983). In our experiment, stimuli were displayed on a fast decay monitor, they were never shown at high contrast and were separated by a blank interval of 100 ms which should have resolved any decay within this temporal window. Moreover, observers were never fully dark-adapted because of the high luminance mask showed at the end of every trial, so that perception of faint phosphor traces caused by persistence is very unlikely. However, to fully rule out any possible contribution from the CRT phosphor persistence, we designed a second experiment.

Experiment 2

To rule out the possibility that the results from Experiment 1 were caused by phosphor persistence, in Experiment 2 stimuli were delivered by an array of ultra-fast LEDs which we had assembled into a custom monitor. The task of the observer was the same of the previous experiment and the procedure was similar. However, there were some important differences between experiments, which are summarized in Figures 5a and d. First, the dimension of the Vernier stimuli were different: in Experiment 2, because of the thickness of the LEDs, the lines were wider and shorter (Fig. 5c). Moreover, because of the structure of the LEDs display, retinal stabilization was only achievable on the horizontal axis. Also the duration of the stimuli presentation differed in the two experiments: in Experiment 2, contrary to Experiment 1, the exposure duration was fixed at 20 ms. This was done to further exclude possible errors in retinal stabilization. Since the time of exposure now always brief and no longer dependent on eye movements, possible spurious retinal image motion was further minimized. Figure 13 summarizes the experimental procedure of Experiment 2.

Data analysis followed the same steps of Experiment 1. The characteristics of ocular drift are shown in Figures 14 and 15. The average speed of ocular drift during the blank interval between the line presentation was 52 ± 6 arcmin/s, a value highly similar to Experiment 1. Again, the preferred direction of ocular drift and its instantaneous velocity was idiosyncratic across observers.

Table II reports the performance of the three observers who took part in this experiment. As expected, for all observers, performance (no horizontal offset between the two bars) was not significantly different from chance level at gap size 0 ($p > 0.05$, CI for binomial distribution). Like in Experiment 1, however, performance increased in all observers with increasing the gap size becoming significantly higher than chance ($p < 0.05$, CI for binomial

distribution).

The data in Table II are reported graphically in Figures 16 and 17. It is clear from these data that all observers were able to perform the task well above chance level even with a gap size of just 1.75'. As shown in Figure 17a in the condition with no horizontal offset between the two line (gap size 0), the average distribution across observers was at chance level (50%). With gap size of 1.75' the average performance increased significantly to 68% in all observers ($p < 0.05$, CI for binomial distribution) and it reached 85% with gap size 3.5'. Figure 17a also reports the average *d'* across observers. The average sensitivity index was 0.93 at gap size 1.7' and it increased to 2.12 with the gap size 3.5' showing that observers has little difficulty performing the task. Results from data collapsed across observers showed identical results for all gap sizes: at 0 it was not significantly different from chance (50%, CI [0.47 0.53]), but it increased with 1.75' (69%, CI [0.65 0.72]) and 3.5' gap size (85%, CI [0.80 0.90]).

As in Experiment 1, the distribution of stabilization errors did not exhibit any obvious link with the subject responses, suggesting that performance was not influenced by possible imprecision in retinal stabilization (Fig. 18). As shown in Figure 17b, subjects were able to correctly report the configuration of the stimulus independently of the direction of drift. These results together with those from Experiment 1 argue against the possibility that results were caused by a general knowledge of the average preferred drift direction. They confirm that the trial-specific displacement caused by ocular drift in the interval between the presentations of the two lines is taken into account in decoding visual signals.

Experiment 3

To rule out the effect of the granularity of the display, a similar issue to Experiment 1, we designed another experiment where stimuli were viewed through a stimulus deflector.

Experiment 4

While the brief flashes of the fast LED ensure that no motion was perceived on the retina, it is still possible that stabilization errors caused by the finite steps of our displays contributed to the results. For this reason, we conducted a third experiment. In this experiment we used for stabilizing the stimulus on the retina a visual stimulus deflector developed by Crane and Steele (1978). This approach enabled the use of high contrast stimuli on a CRT

monitor while simultaneously avoiding confounding effects caused by phosphor persistence. However, because of the time-consuming calibration procedure, this approach allowed data collection only on few highly experienced observers. The experimental design is summarized in Figure 19. The task of the observers was the same as in Experiment 1 and 2, with the Vernier bars displayed for only 20 ms to avoid retinal image motion from possible imperfections in retinal stabilization. Here we considered two conditions which differed in the duration of the interstimulus interval: in the first condition, the blank interval duration was 100 ms, as in Experiments 1 and 2. In a second condition, the duration of the blank interval was increased to 500 ms. This condition was introduced to investigate the temporal limits of the window of integration of extra-retinal information in the visual system. The previous study of Poletti et al. (2010) suggests that this information is not integrated over long intervals. As for the previous experiments, we first report the characteristics of ocular drift and then the performance of the observers in the task.

The general characteristics of ocular drift of the two observers who participated to this experiment are shown in Figures 21 and 20. As noted in previously, ocular drift was idiosyncratic across observers.

Figure 22 shows the results of Experiment 4. In the condition of 100 ms blank interval, both observers had performance at chance level with gap size 0 as show in Figure 22a. Increasing the gap size up to 4', the performance increased significantly above chance level in only for one observer ($p < 0.05$, CI for binomial distribution). However, the performance of both observers was significantly above chance for gap sizes that ranged between 4 and 8' ($p < 0.05$, CI for binomial distribution) . Figure 22b shows the results for both observers with blank interval duration of 500 ms. Neither observers showed performance different from chance level at any gap size range.

The difficulty of the stabilization technique used in Experiment 4 allowed data collection only for a limited amount of highly trained observers. This occurred because the very time-consuming calibration procedure which required skillful cooperation from the subject and left a little time to actual collect data. However, the results confirm that the visual system has access to the information contained in the temporal modulation of ocular drift. Thus, the visual system has knowledge of the main direction of ocular drift also in the absence of any visual cue. This knowledge seems to be available and integrated with visual signals only over a short interval.

Discussion

The results of this study show that fine spatial detail can be represented in time by means of the modulations resulting from fixational eye movements.

In this study, we designed experiments that were testing whether the visual system has access and uses the extra-retinal knowledge of ocular drift. In three experiments, observers could accurately perform the task only if their visual system used an extra-retinal signal providing information about the direction of ocular drift during the 100 ms interstimulus interval. The results show that performance was significantly higher than chance levels even with offsets of few arcmins, demonstrating that the visual system takes full advantage of the "reformatting" of the visual input caused by fixational motion of the retinal image. These results are in agreement with previous theoretical studies (Ahissar and Arieli, 2001, 2012) and extend the findings of previous experimental studies (Rucci et al., 2007; Kuang et al., 2012) showing that the visual system uses the temporal modulation of fixational eye movements to encode fine spatial detail. Interestingly, the 100 ms interstimulus interval was within the range in which humans perceive apparent motion, yet, the observers did not report perceiving apparent motion.

In our experiments subjects were able to detect Vernier offsets as small as 1.35'. This, however, was only possible if the interstimulus interval was short (100 ms). The results of Experiment 4 for the 500 ms interstimulus condition, show that observers were not capable to perform the task accurately with longer intervals. This suggest that the visual system has access to the information of the ocular drift direction for only a limited amount of time. This result is in line with a recent study (Poletti et al., 2010) which showed that spatial representations are not updated by extra-retinal signals. In their experiment observers had to identify which of two test markers was presented at the same position of a reference marker. The test markers were displayed, with intervals of 500 ms, at the same location on the retina and on the display of the reference marker. The performance of the observers drastically decreased increasing the length of ocular drift. Even if in the present Experiment the observers' task was different (observers had to judge the horizontal displacement of two lines) the results point toward a temporal limit in the visual system for knowledge of ocular drift.

The importance of memory in a spatial localization task has been previously described by Matin et al. (1981). In their experiment, observers were asked to perform a Vernier task with lines that were sequentially flashed at different time intervals. As also shown in previous experiments (*e.g.*, Westheimer and McKee, 1975), the

simultaneous presence of the two lines seems to be a prerequisite for optimal performance in Vernier tasks. Matin et al. (1981) argued that eye movements could be a source of error during the interstimulus interval: they concluded that extra-retinal signal was not updated in the representation of the visual system. Their results show that performances decreased increasing the interstimulus intervals. However, in their experiments, contrary to ours, the stimuli were not stabilized on the retina. Therefore, the position of the bars on the retina had to be integrated with the extra-retinal information to accurately perform the task making the task much harder. It would be interesting to investigate in a future experiment the mechanisms of this integration. A Vernier stimulus could be displayed with a retinal offset between two lines sequentially flashed. In this way, it will be possible to better understand the weights of retinal and extra-retinal contributions.

Figures

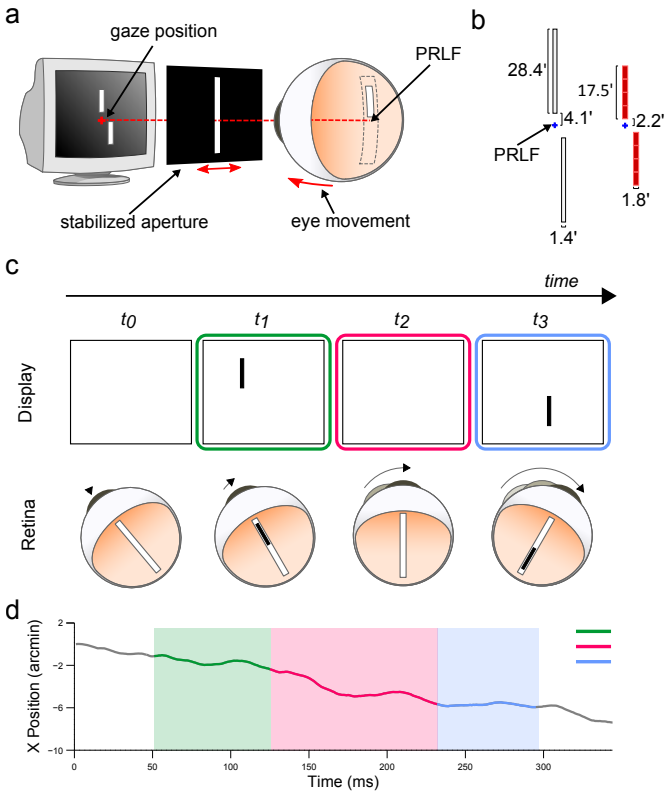

Figure 1: Experimental procedure and stimuli. **a**: A Vernier stimulus viewed through a stabilized aperture. The two lines were never visible simultaneously. **b**: Comparison between the stimuli used in the Experiments 1 and 2. For visualization purpose the two lines are here displaced by 2 pixels gap sizes. The blue cross represents the Preferred Retinal Location of Fixation (PRLF). The two lines are displayed together here only for visualization purpose. **c**: Experimental procedure. Observers are asked to report whether the top bar of a vernier stimulus is to the left or to the right of the bottom one. The two bars are shown at two different temporal interval t_1 and t_3 with a temporal delay (t_2). The two bars of the vernier stimulus are shown at the same horizontal position on the retina aligned with the PRFL, thus no actual displacement is present in the retinal stimulus. **d** INSERT PANEL: example of the horizontal position of the line of sight as a function of time. The green bar represents the temporal interval when the first stimulus was shown (t_1). This period was followed by a blank interval (red, t_2) and the presentation of the second bar (blue, t_3).

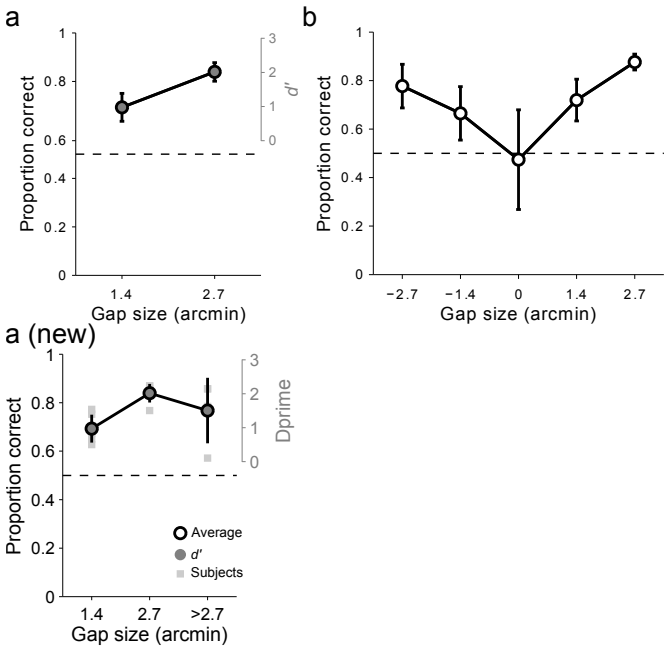

Figure 2: Performance in Experiment 1. **a**: Proportion of correct responses and *d'* as a function of the gap size. The *d'* values are plotted on the right axis (filled data point). **b**: Proportion of correct responses as a function of the gap size according to the main direction of ocular drift. Data represent averages across observers (N = 6). Error bars indicate one standard deviation. **a new**: same data as panel a for gap sizes 1.4' and 2.7'. Data for gap size > 2.7' represent average across observers (N = 4) with at least 20 trials.

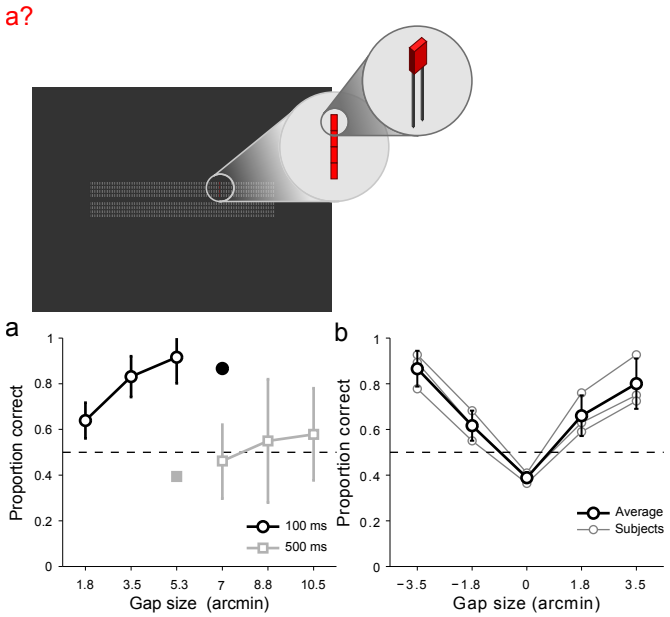

Figure 3: Performance in Experiment 3. **a?**: Schematic representation of the LEDs monitor used in Experiment 2 and 3. **a**: Proportion of correct responses as a function of the gap size for the conditions with 100 and 500 ms interstimulus interval in Experiment 3. **b**: Proportion of correct responses as a function of the gap size according to the main direction of ocular drift for Experiment 3. Data represent averages across observers (N = 3). Error bars indicate one standard deviation. Filled data point represent averages at gap sizes in which observers have less than 10 trials.

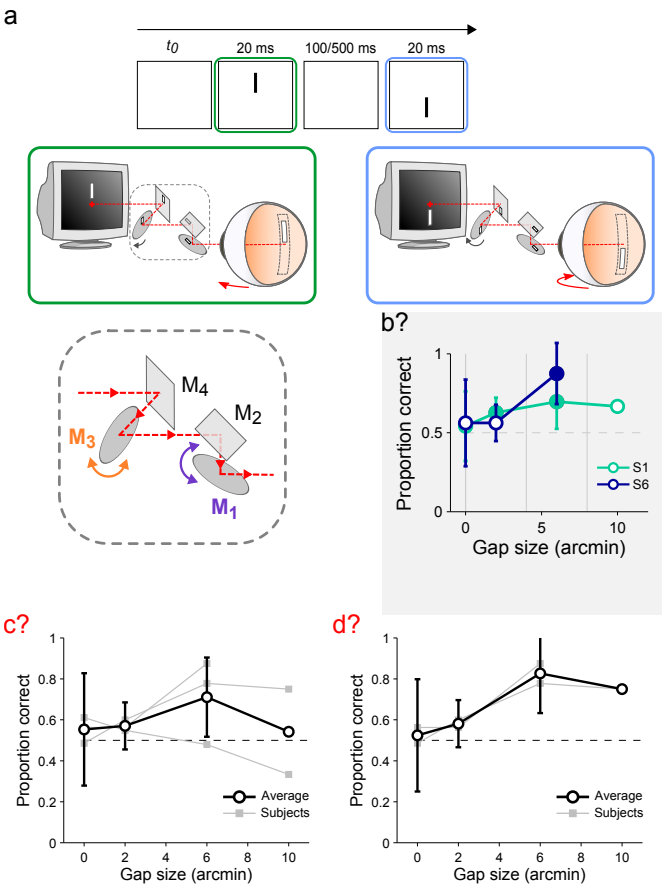

Figure 4: Experimental procedure and performance in Experiment 4. **a**: Schematic representation of the experimental procedure. **b**: Proportion of correct responses as a function of the gap size. Data represent individual observers. Error bars indicate one standard deviation. **c?**: Average performance across observers (N=3). **d?**: Average performance across observers (N=2), same data of panel **b**.

Supplementary material

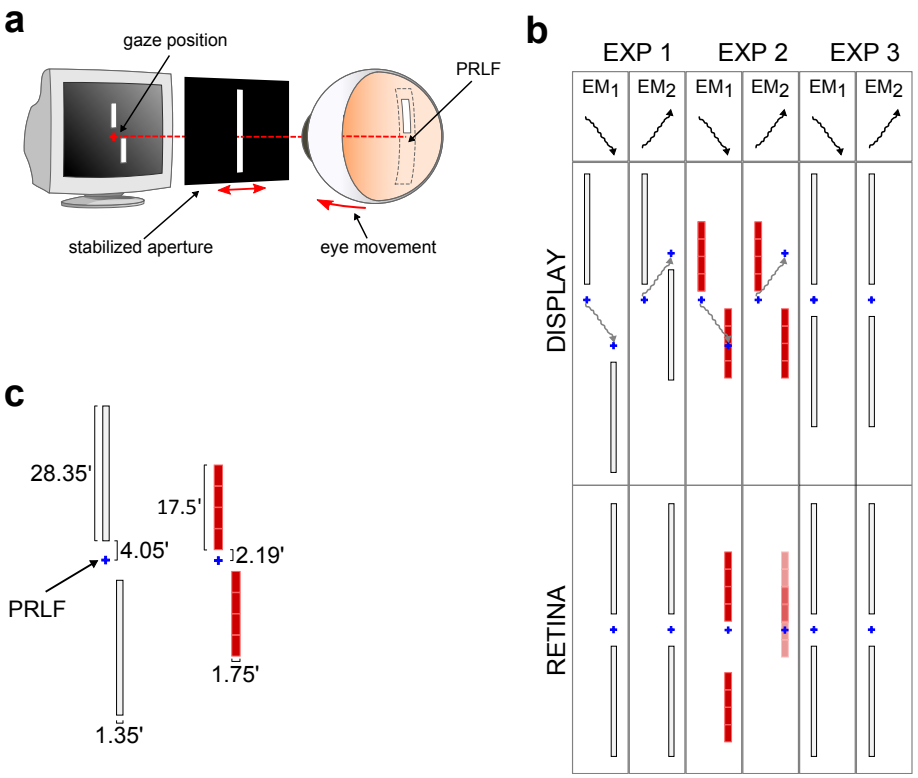

Figure 5: Differences in the retinal stimulus in the three experiments. **a**: A Vernier stimulus viewed through an aperture. The two lines were never visible simultaneously. **b**: Comparison between the configuration of the stimuli on the display and on the retina for the three experiments for two traces of eye movements (EM_1 and EM_2). **c**: Comparison between the stimuli used in the Experiments 1 and 2. For visualization purpose the two lines are here displaced by 2 pixels gap sizes. The blue cross represents the Preferred Retinal Location of Fixation (PRLF). The two lines are displayed together here, but were never visible simultaneously. In all this cases, the temporal configuration of the stimuli was top line first, bottom line second.

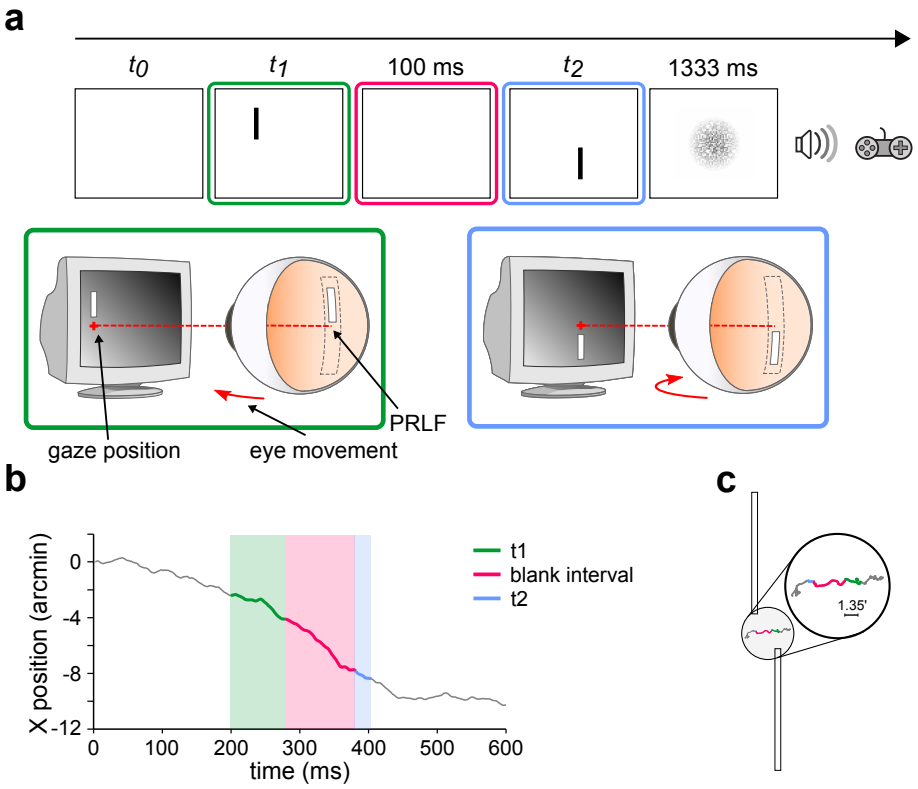

Figure 6: **a**: Schematic representation of the experimental design. Observers had to judge the horizontal displacement of two lines flashed sequentially. The two lines were displayed on the monitor at the current position of the line, so that, they were aligned on the retina. The first stimulus was displayed after a random interval from the beginning of the trial. The two bars were separated by 100 ms blank interval and were displayed for exposure times (t_1) and (t_2), which depended on the observers' eye movements. A jittering random noise mask was shown for 1.3 s to avoid dark adaptation. At the end of the trial (signaled by a tone), observers reported whether the top line was to the left or to the right of the bottom one by pressing a button on a joypad. **b**: Example of the horizontal position of the line of sight as a function of time. The green bar represents the temporal interval when the first stimulus was shown (t_1). This period was followed by a blank interval (red) and the presentation of the second bar (t_2, blue). **c**: 2D visualization of the same trial. Color codes the experimental sequence of the stimuli.

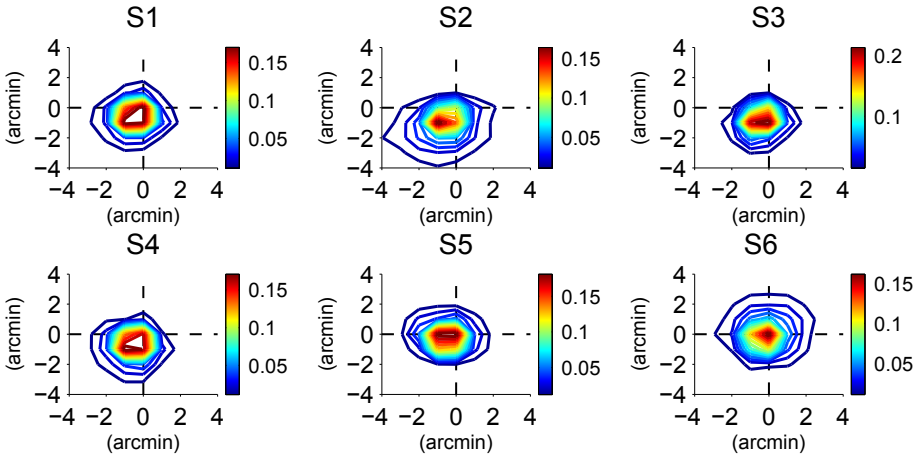

Figure 7: 2D probability distributions of the gaze position during in the 100 ms blank interval between bar exposures in Experiment 1. Each panel shows data from one observer.

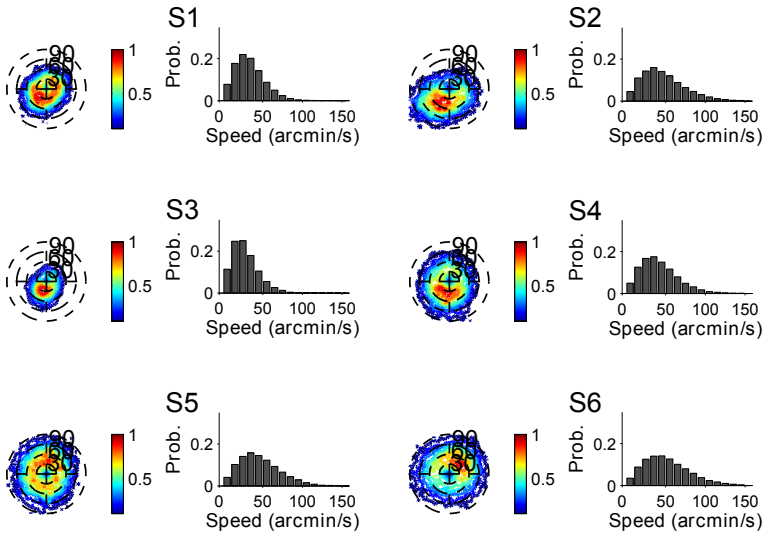

Figure 8: 2D probability distributions of instantaneous velocity and speed (the modulus of the velocity vector) of ocular drift for individual observers in Experiment 1. Maps are in polar coordinates. Color codes the probability of occurrence of instantaneous drift velocity with given direction and amplitude. Each panel shows data from one observer.

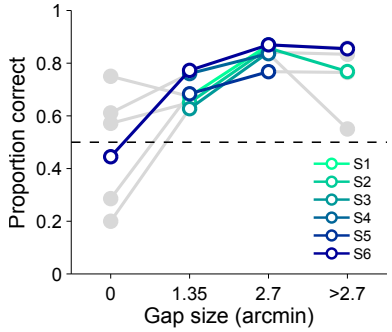

Figure 9: Performance in Experiment 1. Proportion of correct responses as a function of the gap size (direction is collapsed) for each observer. Gray data point represent $N < 30$.

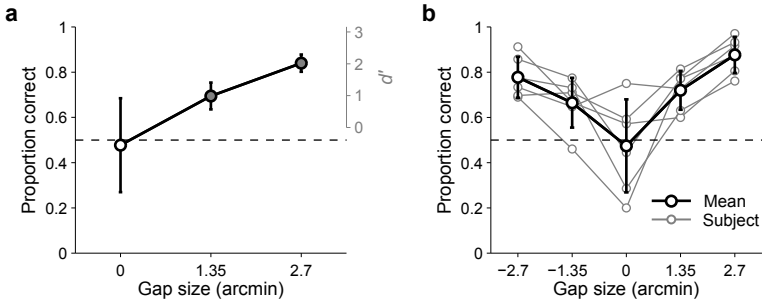

Figure 10: Performance in Experiment 1. **a**: Proportion of correct responses and *d'* as a function of the gap size. The *d'* values for the non-zero gap sizes are plotted on the right axis (filled data points). **b**: Proportion of correct responses as a function of the gap size according to the main direction of ocular drift. Black data represent averages across observers (N = 6). Error bars indicate standard deviations. Gray data point represent individual observers.

		Gap Size			
Subject		**0**	**1.35'**	**2.7'**	**>2.7'**
S1	**Performance**	**75%**	**67%**	**87%**	**86%**
	Number of trials	4	101 (33)	114 (84)	21 (14)
	Number correct trials	3	68 (24)	99 (77)	18 (14)
	CI	- -	[.58 .77]	[.80 .94]	- -
S2	**Performance**	**57%**	**65%**	**86%**	**75%**
	Number of trials	7	60 (15)	70 (36)	60 (16)
	Number correct trials	4	39 (9)	60 (29)	45 (14)
	CI	- -	[.52 .78]	[.77 .94]	[.63 .87]
S3	**Performance**	**20%**	**63%**	**84%**	**83%**
	Number of trials	5	134 (71)	63 (34)	6 (4)
	Number correct trials	1	84 (55)	53 (33)	5 (4)
	CI	- -	[.54 .71]	[.74 .94]	- -
S4	**Performance**	**59%**	**75%**	**83%**	**57%**
	Number of trials	27	105 (43)	77 (44)	21 (4)
	Number correct trials	16	79 (35)	64 (41)	12 (4)
	CI	- -	[.67 .84]	[.74 .92]	- -
S5	**Performance**	**29%**	**68%**	**77%**	**76%**
	Number of trials	21	98 (46)	86 (46)	17 (8)
	Number correct trials	6	67 (29)	66 (35)	13 (7)
	CI	- -	[.59 .78]	[.67 .86]	- -
S6	**Performance**	**44%**	**77%**	**87%**	**85%**
	Number of trials	54	167 (105)	184 (142)	93 (55)
	Number correct trials	24	129 (81)	160 (124)	79 (45)
	CI	[.30 .59]	[.71 .84]	[.82 .92]	[.77 .93]
TOT		**47%**	**69%**	**84%**	**77%**

Table I: Summary of individual results in Experiment 1. For each observer, percentage of correct response, total number of trials, correct trials and confidence intervals are reported for different gap sizes. Number in parenthesis indicate trials to the right. Data for with gap size $> 2.7'$ were collapsed together. CI are calculated only when the number of trials was larger than 30. data in the last column need to be changed!

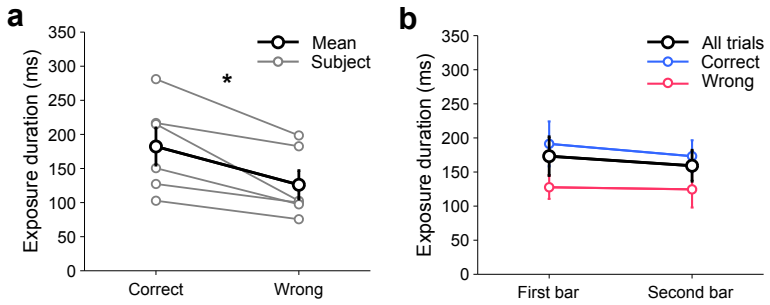

Figure 11: Experiment 1: stimuli exposure duration. **a**: Exposure duration as a function of the response. Gray data represent the average duration for each observer, black data represent averages across observers $\pm$ SEM. $(*)$ $p < 0.01$ (one-sample two-tailed t-test). **b**: Exposure duration as a function of the stimuli order of presentation for all (black), correct (red) and wrong (blue) trials.

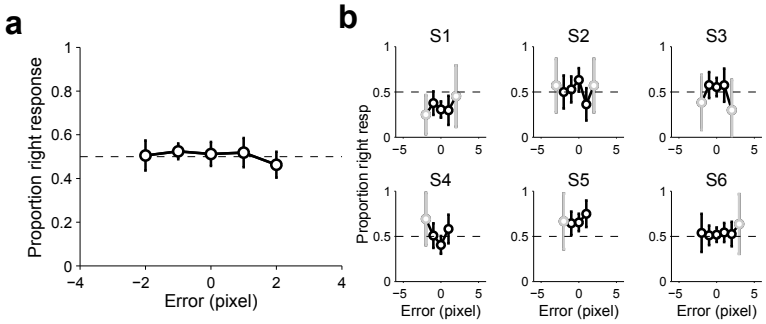

Figure 12: Experiment 1: Retinal error during stabilization. **a**: Proportion of right response (the trials in which observers reported the top bar to be to the left of the bottom bar) response as a function of the offsets caused by retinal stabilization. Retinal errors were calculated as the difference between the average residue of the actual eye and stimuli position of the two intervals during which the stimuli were presented. Data represent averages per bin ± SEM (N per bin >= 4). **b**: Retinal error for each observer. Data represent proportion ± CI. Gray data point show bin where $N < 30$.

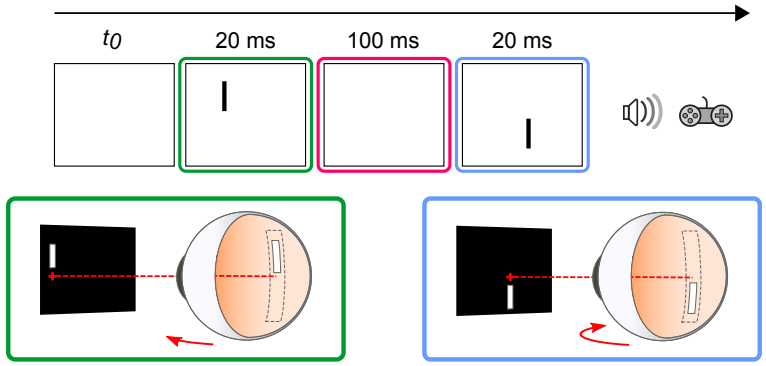

Figure 13: Experiment 2: Schematic representation of the experimental design. Like in Experiment 1, the first stimulus appeared on the monitor vertically aligned with the line of sight after a variable interval and was followed by the second bar after 100 ms interstimulus interval. Unlike Experiment 1, however, both stimuli were displayed for 20 ms only . Subjects reported whether the top bar was to the left or to the right of the bottom one at the end of the trial (signaled by an auditory stimulus) by pressing a button on a joypad.

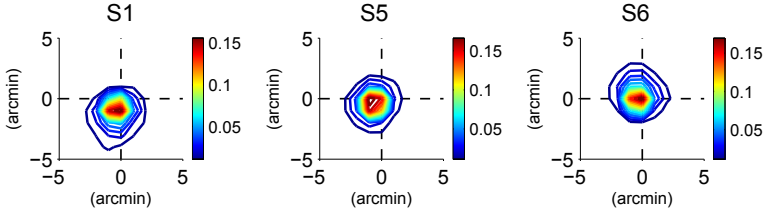

Figure 14: 2D probability distributions of the gaze position during in the 100 ms blank interval between bar exposures in Experiment 2. Each panel shows data from one observer.

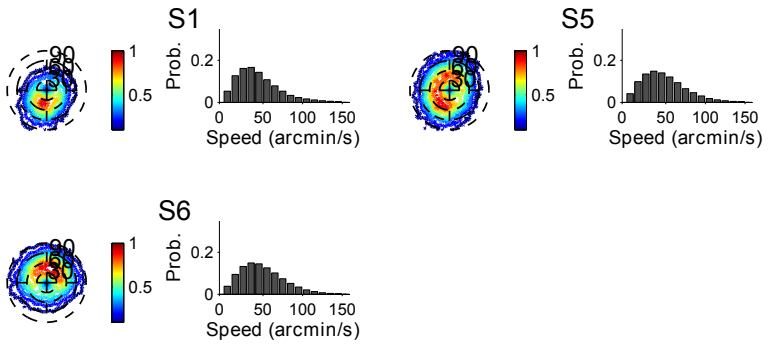

Figure 15: 2D probability distributions of instantaneous velocity and speed (the modulus of the velocity vector) of ocular drift for individual observers in Experiment 2. Maps are in polar coordinates. Color codes the probability of occurrence of instantaneous drift velocity with given direction and amplitude. Each panel shows data from one observer.

		Gap Size			
Subject		**0**	**1.75'**	**3.5'**	**>3.5'**
S1	**Performance**	**54**%	**68**%	**91**%	**83**%
	Number of trials	308	149 (59)	76 (44)	30 (14)
	Number correct trials	165	101 (41)	69 (39)	25 (14)
	CI	[.48 .59]	[.60 .76]	[.84 .98]	[.68 .98]
S5	**Performance**	**50**%	**67**%	**83**%	**67**%
	Number of trials	339	228 (80)	54 (15)	9 (–)
	Number correct trials	169	153 (50)	45 (13)	6 (–)
	CI	[.44 .55]	[.61 .73]	[.73 .94]	- -
S6	**Performance**	**48**%	**69**%	**81**%	**94**%
	Number of trials	481	342 (185)	91 (65)	35 (26)
	Number correct trials	231	237 (119)	74 (49)	33 (24)
	CI	[.44 .53]	[.64 .74]	[.73 .90]	[.85 Inf]
TOT		**50**%	**68**%	**85**%	**88**%

Table II: Experiment 2. Summary of the results in Experiment 2. For each observer, percentage of correct response, total number of trials, correct trials and confidence intervals are reported for different gap sizes. Number in parenthesis indicate trials to the right. Data for with gap size $3.5'$ were collapsed together. CI are calculated only when the number of trials was larger than 30.

		Gap Size			
Subject		**0**	**1.8'**	**3.5'**	**5.3'**
S1	**Performance**	**41**%	**72**%	**93**%	**96**%
	Number of trials	22	94 (50)	82 (41)	26 (14)
	Number correct trials	(9)	68 (38)	76 (38)	25 (13)
	CI	[. .]	[. .]	[. .]	[. .]
S4	**Performance**	**39**%	**62**%	**82**%	**79**%
	Number of trials	28	101 (54)	60 (32)	14 (7)
	Number correct trials	(11)	63 (34)	49 (24)	11 (6)
	CI	[. .]	[. .]	[. .]	[. .]
S5	**Performance**	**36**%	**57**%	**75**%	**100**%
	Number of trials	11	79 (39)	56 (29)	12 (6)
	Number correct trials	(4)	45 (23)	42 (21)	12 (6)
	CI	[. .]	[. .]	[. .]	[. .]
TOT		**39**%	**64**%	**83**%	**92**%

Table III: Experiment 3. Summary of the results in Experiment 3, condition 100 ms. For each observer, percentage of correct response, total number of trials, correct trials and confidence intervals are reported for different gap sizes. Number in parenthesis indicate trials to the right. CI are calculated only when the number of trials was larger than xx. INSERT CI

		Gap Size			
Subject		**5.3'**	**7'**	**8.8'**	**10.5'**
S1	**Performance**	**51**%	**59**%	**59**%	**73**%
	Number of trials	33 (15)	51 (27)	41 (17)	19 (13)
	Number correct trials	17 (7)	30 (17)	24 (11)	14 (7)
	CI	[. .]	[. .]	[. .]	[. .]
S4	**Performance**	**75**%	**52**%	**80**%	**65**%
	Number of trials	4 (3)	23 (17)	20 (9)	17 (9)
	Number correct trials	3 (2)	12 (8)	16 (8)	11 (6)
	CI	[. .]	[. .]	[. .]	[. .]
S5	**Performance**	**27**%	**28**%	**26**%	**35**%
	Number of trials	11 (8)	40 (18)	38 (18)	37 (18)
	Number correct trials	3 (1)	11 (1)	10 (5)	13 (5)
	CI	[. .]	[. .]	[. .]	[. .]
TOT		**51**%	**46**%	**55**%	**58**%

Table IV: Experiment 3. Summary of the results in Experiment 3, condition 500 ms. For each observer, percentage of correct response, total number of trials, correct trials and confidence intervals are reported for different gap sizes. Number in parenthesis indicate trials to the right. CI are calculated only when the number of trials was larger than xx. INSERT CI

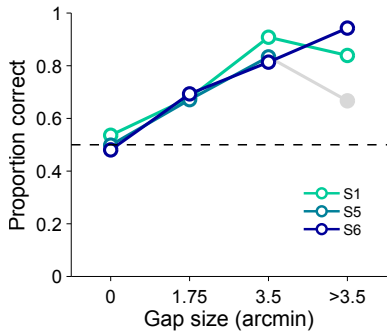

Figure 16: Performance in Experiment 2. Proportion of correct responses as a function of the gap size (direction is collapsed) for each observer. Gray data point represent $N < 30$.

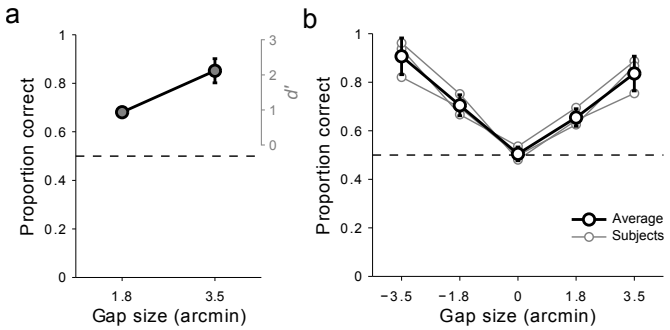

Figure 17: Performance in Experiment 2. **a**: Proportion of correct responses and *d'* as a function of the gap size. The *d'* values for the non-zero gap sizes are plotted on the right axis (filled data points). **b**: Proportion of correct responses as a function of the gap size according to the main direction of ocular drift. Black data represent averages across observers (N = 3). Error bars indicate standard deviations. Gray data point represent individual observers.

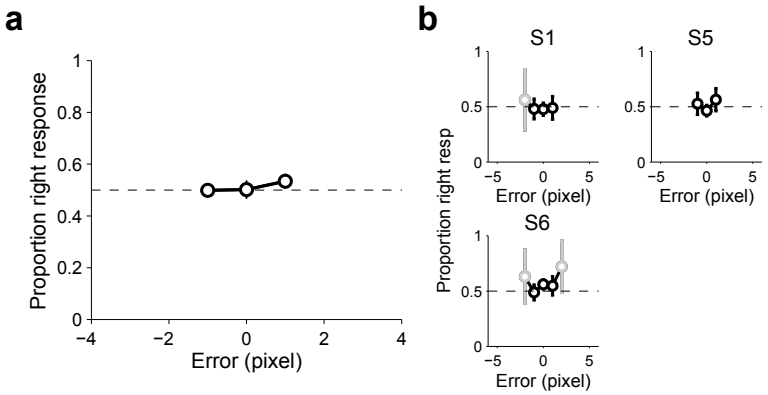

Figure 18: Experiment 2: Retinal error during stabilization. **a**: Proportion of right response (the trials in which observers reported the top bar to be to the left of the bottom bar) response as a function of the offsets caused by retinal stabilization. Retinal errors were calculated as the difference between the average residue of the actual eye and stimuli position of the two intervals during which the stimuli were presented. Data represent averages per bin $\pm$ SEM). **b**: Retinal error for each observer. Data represent proportion $\pm$ CI. Gray data point show bin where $N < 30$.

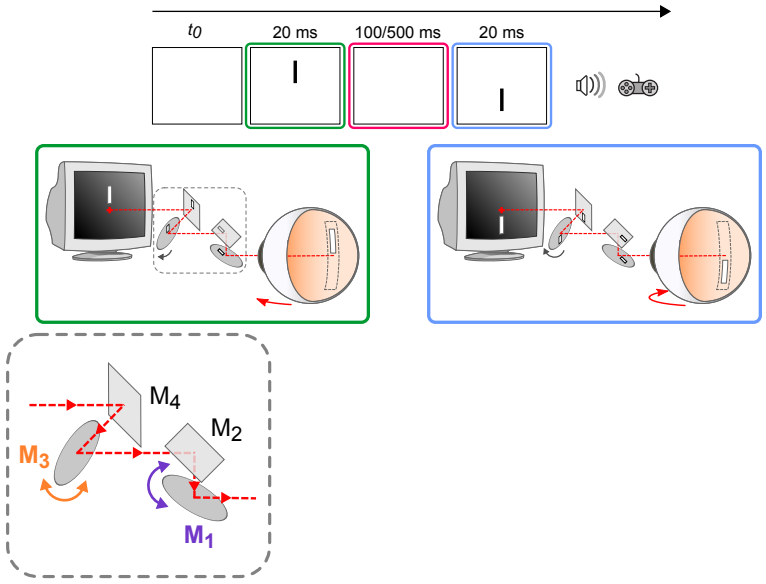

Figure 19: Experiment 4: Schematic representation of the experimental design. After a variable interval the first stimulus was displayed at the center of the monitor vertically aligned with the line of sight for 20 ms. After a blank interval of either 100 or 500 ms, the second stimulus was displayed also for 20 ms. Subjects reported whether the top bar was to the left or to the right of the bottom one at the end of the trial (signaled by an auditory stimulus) by pressing a button on a joypad. M2 and M4: rotating horizontal and vertical deflector mirrors. M1 and M3: stationary mirrors.

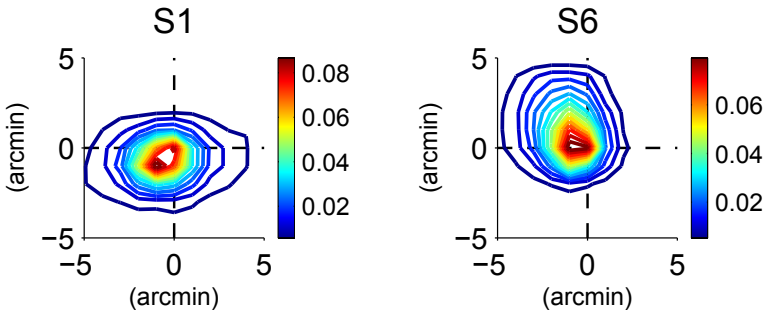

Figure 20: 2D probability distributions of the gaze position during in the 100 ms blank interval between bar exposures in Experiment 3. Each panel shows data from one observer.

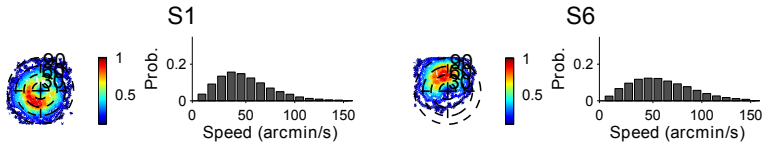

Figure 21: 2D probability distributions of instantaneous velocity and speed (the modulus of the velocity vector) of ocular drift for individual observers in Experiment 3. Maps are in polar coordinates. Color codes the probability of occurrence of instantaneous drift velocity with given direction and amplitude. Each panel shows data from one observer.

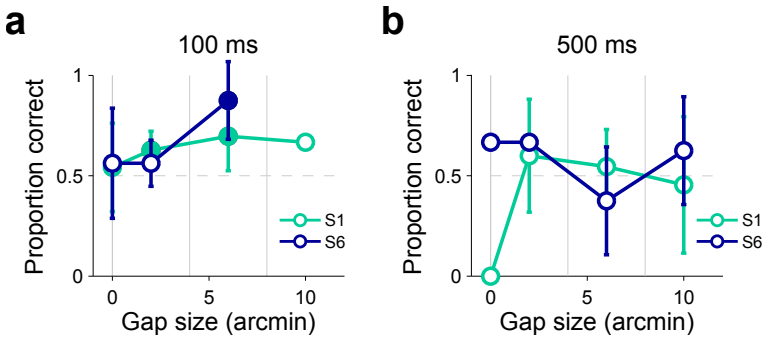

Figure 22: Performance in Experiment 4. Proportion of correct responses as a function of the gap size (direction is collapsed) for each observer. Data represent proportion $\pm$ CI for each individual observer. **a:** 100 ms blank interval condition. **b:** 500 ms blank interval condition. Filled data point represent $p < 0.05$, CI from binomial distribution.

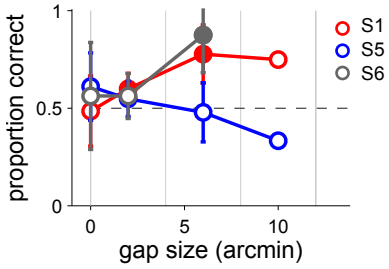

Figure 23: Performance in Experiment 4. Proportion of correct responses as a function of the gap size (direction is collapsed) for each observer. Data represent proportion $\pm$ CI for each individual observer. Filled data point represent $p < 0.05$, CI from binomial distribution.

References

Ahissar, E. and Arieli, A. (2001). Figuring space by time. *Neuron*, 32:185–201.

Ahissar, E. and Arieli, A. (2012). Seeing via miniature eye movements: A dynamic hypothesis for vision. *Frontiers in Computational Neuroscience*, 6.

Arathorn, D., Stevenson, S., Yang, Q., Tiruveedhula, P., and Roorda, A. (2013). How the unstable eye sees a stable and moving world. *Journal of Vision*, 13(10):1–19.

Averill, H. I. and Weymouth, F. W. (1925). Visual perception and retinal mosaic, II. The influence of eye movements on the displacement threshold. *Journal of Comparative Psychology*, 5(2):147–176.

Barlow, H. (1979). Reconstructing the visual image in space and time. *Nature*, 279:189–190.

Brenner, E. and Smeets, J. B. (2000). Motion extrapolation is not responsible for the flash-lag effect. *Vision research*, 40(13):1645–8.

Burr, D. and Ross, J. (1986). Visual processing of motion. *Trends in Neurosciences*, 9(July):304–307.

Burr, D. C. (1979). Acuity for apparent vernier offset. *Vision research*, 19(7):835–7.

Cherici, C., Kuang, X., Poletti, M., and Rucci, M. (2012). Precision of sustained fixation in trained and untrained observers. *Journal of vision*, 12(6):1–16.

Crane, H. D. and Clark, M. R. (1978). Three-dimensional visual stimulus deflector. *Applied Optics*, 17(5):706–14.

Crane, H. D. and Steele, C. M. (1978). Accurate three-dimensional eyetracker. *Applied optics*, 17(5):691–705.

Crane, H. D. and Steele, C. M. (1985). Generation-V dual-Purkinje-image eyetracker. *Applied Optics*, 24(4):527.

Deubel, H. and Bridgeman, B. (1995). Fourth Purkinje image signals reveal eye-lens deviations and retinal image distortions during saccades. *Vision Research*, 35(4):529–38.

Hering, E. (1899). Über die Grenzen der Sehschärfe. *Berichte über die Verhandlungen der Königlich-Sächsischen Gesellschaft der Wissenschaften zu Leipzig, Mathematisch-Physische Classe; Naturwissenschaftlicher Teil*, pages 16–24.

Irwin, D. E., Yantis, S., and Jonides, J. (1983). Evidence against visual integration across saccadic eye movements. *Perception & psychophysics*, 34(1):49–57.

Jonides, J., Irwin, D. E., and Yantis, S. (1982). Integrating Visual Information from Successive Fixations. *Science*, 215(4529):192–194.

Krekelberg, B. and Lappe, M. (1999). Temporal recruitment along the trajectory of moving objects and the perception of position. *Vision Research*, 39(16):2669–79.

Kuang, X., Poletti, M., Victor, J. D., and Rucci, M. (2012). Temporal encoding of spatial information during active visual fixation. *Current biology : CB*, 22(6):510–4.

Marshall, W. H. and Talbot, S. A. (1942). Recent evidence for neural mechanisms in vision leading to a general theory of sensory acuity. In *Biological Symposia - Visual mechanisms, volume 7*, pages 117–164. Cattel, Lancaster, PA, h. kluver edition.

Matin, L., Pola, J., Matin, E., and Picoult, E. (1981). Vernier discrimination with sequentially-flashed lines: roles of eye movements, retinal offsets and short-term memory. *Vision research*, 21(5):647–56.

Morgan, M. J. (1979). Perception of continuity in stroboscopic motion: a temporal frequency analysis. *Vision research*, 19(5):491–500.

Poletti, M., Listorti, C., and Rucci, M. (2010). Stability of the visual world during eye drift. *The Journal of neuroscience : the official journal of the Society for Neuroscience*, 30(33):11143–50.

Purushothaman, G., Patel, S. S., Bedell, H. E., and Ogmen, H. (1998). Moving ahead through differential visual latency. *Nature*, 396(6710):424.

Rucci, M., Iovin, R., Poletti, M., and Santini, F. (2007). Miniature eye movements enhance fine spatial detail. *Nature*, 447(7146):851–4.

Schlag, J. and Schlag-Rey, M. (2002). Through the eye, slowly: delays and localization errors in the visual system. *Nature Reviews Neuroscience*, 3(3):191–215.

Stevenson, S. B. and Roorda, A. (2005). Correcting for miniature eye movements in high resolution scanning laser ophthalmoscopy. In Manns, F., Soederberg, P. G., Ho, A., Stuck, B. E., and Belkin, M., editors, *Biomedical Optics*, pages 145–151.

Westheimer, G. and Hauske, G. (1975). Temporal and Spatial Interference with Vernier Acuity. *Vision Research*, 15:1137–1141.

Westheimer, G. and McKee, S. P. (1975). Visual acuity in the presence of retinal-image motion. *Journal of the Optical Society of America*, 65(7):847–50.

Whitney, D. and Murakami, I. (1998). Latency difference, not spatial extrapolation. *Nature Neuroscience*, 1(8):656–7.